Vol 1, 1 (2015) 12-18

Contents lists available at Article URL

KKU Journal of Basic and Applied Sciences

Journal homepage: jbas.kku.edu.sa

The design of diazienyl derivatives as potential corrosion inhibitors of steel: A structure-activity relationship

Abdullah G. Al-Sehemi[a,b,c], Ahmad Irfan[a*], Shabbir Muhammad[d] and Abul Kalam[a]

[a] Department of Chemistry, Faculty of Science, King Khalid University, Abha 61413, P.O. Box 9004, Saudi Arabia
[b] Unit of Science and technology, Faculty of Science, King Khalid University, Abha 61413, P.O. Box 9004, Saudi Arabia
[c] Research Center for Advanced Materials Science, King Khalid University, Abha 61413, P.O. Box 9004, Saudi Arabia
[d] Department of Physics, Faculty of Science, King Khalid University, Abha, Saudi Arabia

Received: 23 August 2014 / Revised: 11 November 2014 / Accepted: 5 February 2015/ Published: 20 March 2020

Abstract: In present investigation, we have designed several novel corrosion inhibition compounds using diazenyl as central core while pyrazole-5-one and substituted phenyl as lateral moieties (hereafter will be called diazenyl derivatives). The ground state geometries of diazenyl derivatives have been optimized by using density functional theory (DFT) methods with three different basis sets i.e. 6-31G*, 6-311G** and 6-311++G**. The inhibition efficiency of different diazenyl derivatives has been calculated to determine the relationship between their molecular structures and inhibition activity. The calculated efficiencies have also compared with some standard organic inhibitors. Several quantum chemical parameters, specifically, E_{HOMO} (highest occupied molecular orbital energy), E_{LUMO} (lowest unoccupied molecular orbital energy), the energy difference between E_{HOMO} and E_{LUMO} (Δ E), dipole moment (μ), electron affinity (EA), ionization potential (IP), the absolute electronegativity (χ), absolute hardness (η), softness (Σ), Mulliken charges, and the fraction of electrons (ΔN) transfer from inhibitors to iron were calculated and correlated. We have also shed light on the polarizabilty, static first hyperpolarizability (β_{tot}) and its components.

Keywords: Corrosion inhibition; Density Functional Theory; Time dependent density functional theory; Electronic properties; Molecular properties.

1. INTRODUCTION

The metallic infrastructure of many industries is often prone to corrosion, which cause many disadvantages ranging from loss of materials to chemical contaminations that can pose several financial, environmental and health risks. Many industries are spending millions of dollars to avoid the unwanted process of corrosion. Among several techniques that have been applied to reduce the corrosion of metals, the use of corrosion inhibitors is a very common method for protection of metals against corrosion in acidic media[1-3]. Corrosion inhibitors can be classified into three kinds: (i) inorganic inhibitors, (ii) organic inhibitors, and (iii) mixed material inhibitors [4]. Several studies have examined the relationship between the structure of the inhibitor molecule and its efficiency[5-9]. Initially, to cope with corrosion, several neutralizers have been used by the industry for example sodium hydroxide, ammonium and sodium carbonates etc. But with the passage of time these have been replaced with organic inhibitors available in many soluble forms. The working of organic inhibitors usually involves the protection of the metal surface from corrosion by forming a film on the metal surface[10]. The real time efficiency of an organic inhibitor depends on many factors including its electronic structure, chemical composition, surface charge density as well as its affinity toward metal surface[11-14]. Several organic inhibitors with heteroatoms like nitrogen, oxygen, sulphur and phosphorus show more effective interaction with metal surfaces because of the presence of their free electrons pairs. A thorough review of literature exhibits that organic compounds contain nitrogen, oxygen, sulphur and/or aromatic ring in their molecular structure are usually employed as corrosion inhibitors[15,16].

In present study, we have spotlighted the diazenyl derivatives as organic inhibition compounds of interest, see scheme 1. These compounds are expected to be excellent corrosion inhibitors because of the presence of hetro-atoms like nitrogen, carbon and oxygen atoms in them. Experimental means are often expensive and time-consuming to explain and investigate the mechanism of corrosion inhibition. Recently, many academic and industrial laboratories have started the use of advanced and high-performance computers and softwares to study the corrosion inhibition process[17]. Quantum chemical methods are usually applied to study the relationship between the inhibitor molecular properties and their corrosion inhibition efficiencies. However, so far no quantum chemical study has been reported about the study of

Correspondence:
irfaahmad@gmail.com
Tel: o*******

diazenyl derivatives. In this work, the structural, electronic and molecular properties of diazenyl derivatives were investigated at density functional theory level. Our aim is to shed light on the corrosion inhibition activity by calculating several chemical descriptors, e.g. electron affinity (EA),

ionization potential (IP), the absolute electronegativity (χ), absolute hardness (η), softness (Σ) and the fraction of electrons (ΔN) transfer from inhibitors to iron. We have also shed light on the polarizabilty, static first hyperpolarizability (β_{tot}) and its components. The present study deals with the effect of donor and acceptor groups on the corrosion inhibition. This study would also help the experimentalists to synthesize new corrosion inhibitors.

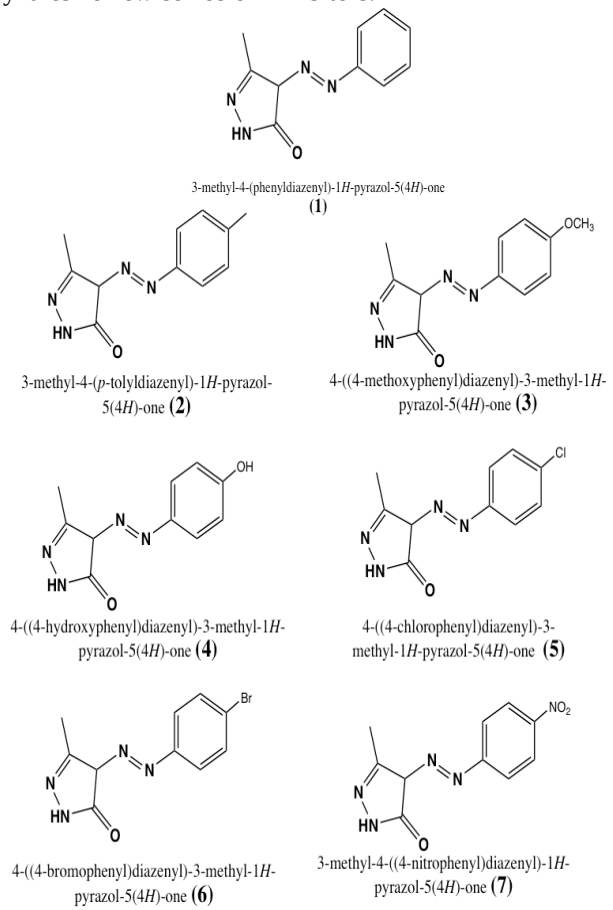

Scheme 1. The schematic representation of designed *diazenyl derivatives* and their chemical names.

2. COMPUTATIONAL DETAIL

All calculations were performed by Gaussian 09 software. The density functional theory (DFT) method has been used to calculate geometries and other electronic properties of above presented compounds. The B3LYP delivers the best depiction among the standard DFT functionals, which is a good choice for small molecules as in present study[18-28]. Using B3LYP method maximum absorption wavelengths of numerous organic dyes (hydrazone, azobenzene, anthraquinone, phenylamine and indigo) have been computed and found good agreement with the experimental data (deviation almost 0.20 eV)[29]. Recently, we showed that the computed electronic and charge transport properties of dianthra [2,3-b:20,30-f]thieno[3,2-b] thiophene at B3LYP/6-31G** level of theory were in good agreement with the experimental values[26]. More recently, B3LYP has been applied to compute the properties of interests which reproduced the promising experimental evidences e.g., hydrazones[30], triphenylamine dyes[31], chemosensors[32], phthalocyanines[33], biologically active molecules[34], and oxadiazoles[35]. In the present investigation, ground state geometries were optimized at the B3LYP/6-31G*, B3LYP/6-311G** and B3LYP/6-311++G** level of theories. The DFT based reactivity descriptors were calculated by using eq. (3) to (6). These structure-property descriptors play an important role to study the reactivity of corrosion inhibitors[36] .

Mulliken electronegativity (χ), hardness (η), and chemical softness (Σ) were calculated from the following equations:

$\chi = (E_{HOMO} + E_{LUMO})/2$ (1)

Hardness (η) was defined as:

$\eta = (E_{LUMO} - E_{HOMO})/2$ (2)

Softness (Σ) was calculated as:

$\Sigma = 1/2\eta$ (3)

Similarly, electrophilicity index (ωi) was calculated using hardness value with the help of following equation:

$\omega i = \mu^2/2\eta$ (4)

The Koopmans' launches the relation between E_{HOMO}/E_{LUMO} and ionization potential (IP) / electron affinity (EA)[37] which can be calculated by the following equations.

$IP = - E_{HOMO}$ (5)

$EA = - E_{LUMO}$ (6)

3. RESULTS AND DISCUSSIONS

Molecular Geometries

The geometrical parameters computed at B3LYP/6-31G*, B3LYP/6-311G** and B3LYP/6-311++G** level of theories have been given in Table 1. To see the effect of basis set, we have applied three basis sets including 6-31G*, 6-311G** and 6-311+G** with different balance of polarization and diffuse functions. The bond length of 1.253Å for N7-N8 bond shows slight variation by shortening to 1.246Å for higher basis sets of 6-311G** and 6-311+G**. The rest of the bond lengths and bond angles at all the level of theories are semi-quantitatively similar showing that basis set has no significant effect on the geometrical parameters. The optimized molecular structure is not linear in one plan due to the slight bent of pyrazole-5-one and diazenyl moiety. The optimized structure of system 1 (see Fig. 1) shows that the oxygen atom of pyrazole-05-one is pointing towards the diazenyl moiety in its minimum energy structure.

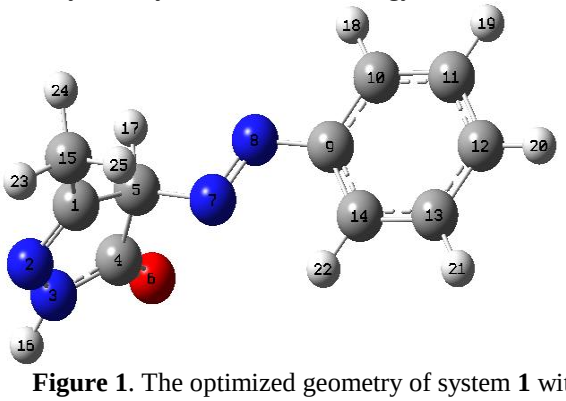

Figure 1. The optimized geometry of system **1** with its labeled atoms.

Systems	1	2	3	4	5	6	7
*B3LYP/6-31G**							
C11-C12	1.396	1.399	1.404	1.400	1.394	1.393	1.393
C12-C13	1.401	1.408	1.406	1.405	1.400	1.399	1.397
C9-N8	1.425	1.422	1.417	1.417	1.423	1.423	1.428
N7-N8	1.253	1.254	1.256	1.256	1.254	1.254	1.252
C11-C12-C13	120.15	118.32	119.91	120.22	121.42	121.45	122.34
N7-N8-C9	114.99	115.04	115.31	115.26	114.83	114.82	114.44
*B3LYP/6-311G***							
C11-C12	1.393	1.397	1.402	1.397	1.391	1.391	1.389
C12-C13	1.398	1.406	1.404	1.403	1.396	1.397	1.394
C9-N8	1.425	1.422	1.416	1.416	1.423	1.423	1.427
N7-N8	1.246	1.247	1.249	1.248	1.246	1.246	1.245
C11-C12-C13	120.15	118.32	119.81	120.11	121.47	121.46	122.35
N7-N8-C9	115.36	115.41	115.68	115.63	115.19	115.18	114.80
*B3LYP/6-311++G***							
C11-C12	1.393	1.397	1.400	1.396	1.391	1.391	1.390
C12-C13	1.399	1.406	1.405	1.402	1.397	1.397	1.395
C9-N8	1.426	1.422	1.418	1.418	1.424	1.424	1.429
N7-N8	1.245	1.246	1.248	1.247	1.245	1.245	1.244
C11-C12-C13	120.13	118.29	119.70	120.27	121.42	121.43	0.971
N7-N8-C9	115.62	115.68	115.75	115.88	115.47	115.45	1.361

Table 1: The bond lengths (*Å*) and bond angles (degree) of system 1 at B3LYP functional and three different basis sets. The labeling of atoms is according to Fig. 1.**Molecular properties**

The HOMOs are delocalized at pyrazole moiety and bridge while LUMOs are localized at diazenyl side and bridge in **1**, **2**, **5-7** revealing intra-molecular charge transfer within the systems. In **3**, the HOMO/LUMO is delocalized/localized on entire of the system. In **4**, almost similar distribution for HOMO has been observed like the **3** while in LUMO some of the ICT can be seen from pyrazole moiety to rest of the system, see Fig. 2.

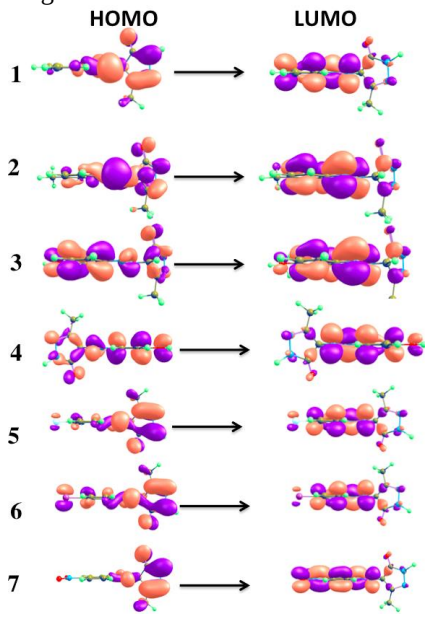

Figure 2. The distribution pattern of the HOMOs and LUMOs of all studied compounds

The frontier molecular orbitals (FMOs) play a very crucial role in the reactivity of any molecule. Among FMOs, highest occupied molecular orbital (HOMO) and lowest unoccupied molecular orbital (LUMO) are very important. These molecules determine the way that it interacts with other species. The HOMO energies (E_{HOMO}), LUMO energies (E_{LUMO}), HOMO–LUMO energy gaps (E_{gap}), χ, η, Σ and ωi at the B3LYP/6-31G*, B3LYP/6-31+G*, B3LYP/6-311G* and B3LYP/6-311++G** level of theories have been presented in Table 2. It has been observed that the trend of the E_{HOMO}, E_{LUMO}, E_{gap}, χ, η, ω, Σ and ωi at all the level of theories is similar. The resistance to charge transfer can be measured by η values. The stabilization energy can be discussed on the basis of ωi which governs the affinity for the electrons. Generally, the electron donor group (**2-4**) lowered while electron-withdrawing group (**5-7**) increased the χ, and ωi compared to phenyl substituted derivative (**1**).

The HOMO is generally concomitant with the electron donating capability of the molecule. High E_{HOMO} values reveal that the molecule has affinity to donate electrons to applicable acceptor molecules. The adsorption can be facilitated by increasing the E_{HOMO} values (and therefore inhibition) by impelling the transport process through the adsorbed layer. The E_{LUMO} designates the aptitude of the molecules to accept electrons. If E_{LUMO} would be lower than the molecule might consent electrons more efficiently[38]. Moreover, smaller E_{gap} contributes worthy inhibition efficiencies as the energy to remove electron from the last occupied molecular orbital will be low[38]. In Table 2, we listed the calculated energies for the E_{HOMO}, E_{LUMO} and E_g for the studied compounds at ground states. The trend of E_{HOMO} is as follows: **3** > **4** > **2** > **1** > **6** > **5** > **7**. The tendency in E_{LUMO} is as: **3** > **4** > **2** > **5** = **6** > 1 > **7**. The trend of E_g is **2** > **1** > **5** > **6** = **4** > **3** > **7**. The system **3** has the highest E_{HOMO} while the lowest E_{LUMO} has been observed for **7**. Another point to be considered is the E_{gap}; the smaller E_{gap} have been observed for the **7** and **3** among all the systems. It is revealing that systems **7** and **3** have more preference to get adsorbed on the metal surface.

The electronic charge density on the chelating atom play important role towards the atom binding ability of a molecule with the metal. The atomic charge values acquired by the Mulliken population analysis showed good and rational manner[39]. In the present study, we have tabulated the Mulliken charges of all the atoms in Table S1. From the atomic charge values listed, N2, N3, O6, N7 and N8 atoms.

Table 2: Different chemical descriptors for all adopted systems (**1-7**) obtained at B3LYP/6-31G* level of theory.

Sys.	1	2	3	4	5	6	7
E_{HOMO} (eV)	-6.47	-6.39	-6.09	-6.19	-6.62	-6.60	-6.88
E_{LUMO} (eV)	-2.80	-1.99	-1.87	-1.90	-2.31	-2.31	-3.10
E_{gap} (eV)	4.39	4.40	4.22	4.29	4.31	4.29	3.78
I.P (eV)	6.47	6.39	6.09	6.19	6.62	6.60	6.88
EA (eV)	2.80	1.99	1.87	1.90	2.31	2.31	3.10
χ	4.28	4.19	3.98	4.04	4.46	4.46	4.99
η	5.43	5.40	5.16	5.24	5.46	5.44	5.33
Σ	0.18	0.19	0.19	0.19	0.18	0.18	0.19
ωi	1.68	1.63	1.54	1.56	1.82	1.82	2.33
ΔN	0.251	0.260	0.293	0.282	0.232	0.234	0.189
ΔE	-1.357	-1.349	-1.289	-1.310	-1.366	-1.361	-1.332

Table 3: The calculated values of dipole moments (μ), static polarizability (α_0), anisotropy (Δα), static first hyperpolarizability (β_0), and total first hyperpolarizability (β_{tot}) for all adopted systems at B3LYP/6-31G* level of theory

Property	1	2	3	4	5	6	7
μ (D)	3.06	3.39	3.91	3.48	2.83	2.81	4.94
α_0 (a.u.)	138	154	162	147	155	163	160
Δα (a.u.)	112	131	144	130	144	157	144
β_0 (a.u.)	94	368	1095	832	669	886	1639
β_{tot} (a.u.)	158	613	1825	1387	1115	1478	2732

of system **3** have excess electron density, more significant charge density has been observed on N7 (-0.1518) which increases the p-electron density in the aromatic ring whilst in all other studied compounds these atoms less contribute to the p-system when compared to **3**. It is well-known that more negative charge would lead to the stronger binding ability thus it is expected that **3** would be easier to bind with metal.

To shed light on the structure and electronic distribution in a molecule the dipole moment (μ) has been investigated. Moreover, in previous studies there is a lack of agreement on the correlation between the μ and inhibition efficiency[40,41]. Popova and co-workers pointed out that the increasing values of μ would facilitate adsorption[42]. In literature, we can find that the inhibition efficiency increases with increasing values of the μ[43]. Instead, some studies showed irregularities in case of correlation between μ *and* inhibition efficiency[44]. In the present case highest μ have been observed for **7** and **3**. We didn't find substantial relationship between the μ values and inhibition efficiencies. The system **3** has the highest μ value among all the systems except system **7**, see Table 3.

Fraction of transferred electrons (ΔN)

We have computed the fraction of electrons transferred from the inhibitor molecule to the metallic atom (ΔN) according to Pearson[45]. They highlighted that in two systems having different electronegativities (as a metallic surface and an inhibitor molecule) electrons would flow from low χ towards the higher value till chemical potentials are same. With the intention of computing the ΔN, we have used theoretical value for the χ of bulk iron χ_{Fe}= 7 eV[45], and a global hardness of η_{Fe} = 0, by assuming that for a metallic bulk IP = EA[46] because they are softer than the neutral metallic atoms. The following formula has been used to compute the ΔN[45]:

$$\Delta N = \chi_{Fe} - \chi_{inb} / 2(\eta_{Fe} + \eta_{inh}) \qquad (7)$$

The lowest η and χ values have been observed for **3** see Table 2. The highest ΔN has been observed for the **3** as compared to the other investigated compounds. Lece and coauthors showed that low η and high ΔN values improves the inhibition efficiency. Thus, the higher inhibition of **3** may be ascribed to the substitution of $–OCH_3$. Furthermore, organic inhibitors containing reactive functional groups would be favorable positions of the adsorption process. The electron density of the donating atom also play vital role on the strength of the adsorption bond[17]. The inhibition efficiency can be improved by substituting the mercapto group to a heterocyclic compound[47]. The superior inhibition efficiency of **2** and **4** compared to **1**, **5**-**7** is due to the presence of $-CH_3$ and -OH groups in **2** and **4**, respectively. The electron donor groups ($-OCH_3$, -OH, $-CH_3$) increases the electron density which is also a factor to improve the inhibition efficiency.

Absorption Spectra

To investigate the electronic transition nature, we have applied the time dependent density functional theory (TD-DFT) approach. The accurate absorption wavelength at relatively small computing time can be easily detect by TD-DFT study, which corresponds to vertical electronic transitions computed on the basis of ground state geometry[48]. The excitation energies, absorbance and oscillator strengths for diazenyl molecules at the optimized geometries in the ground state were obtained in the frame work of TD-B3LYP/6-31G* level of theory. The significant effect of EWDG ($-NO_2$) has been observed towards the red shift in the absorption wavelengths. In phenyl substituted derivative (**1**), three absorption spectrum peaks have been observed at 245, 267 and 302 nm. By substituting the donor group (**2**-**4**) the second peak intensity (at 272 nm) decreases. By introducing the $–OCH_3$, 24 nm red shift has been observed in the maximum absorption wavelength compared to the **1**. Moreover, in chloro (**5**) and bromo (**6**) substituted derivatives three absorption wavelengths have been observed but no significant effect of EWDGs have been noticed on the absorption wavelengths towards red/blue shift. In **7**, two absorption wavelengths have been observed; by introducing the $-NO_2$ increased the second peak intensity (at 282 nm) and 40 nm red shift was noticed in the maximum absorption wavelength compared to **1**, see Fig. 3.

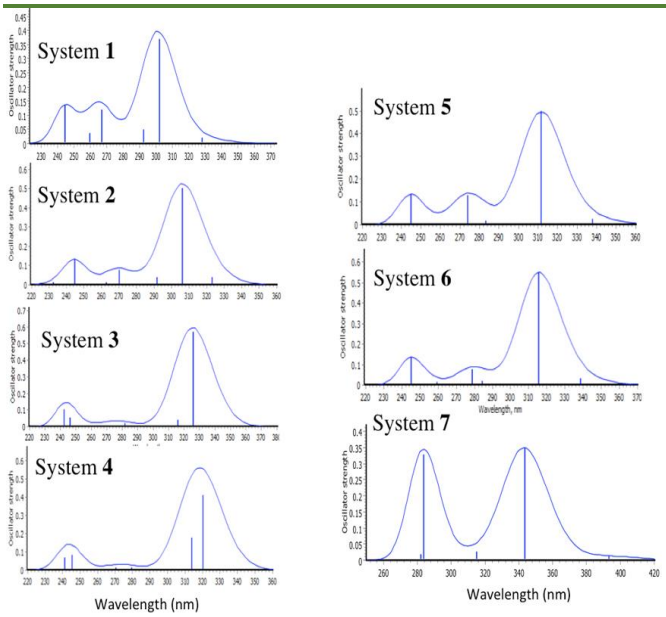

Figure 3. The absorption spectra of investigated compounds in the present study

Polarizability and first hyperpolarizability

The Finite Field (FF) method has been used to calculate the static first hyperpolarizability (β_{tot}) and its components for all diazenyl derivatives. The FF methodology has been applied to calculate first hyperpolarizability because this method has given good semi-quantitative results in concert with the electronic structure method[49]. In FF approach, the energy (E) of a molecule is expressed by Eq.1, when it is subjected to a static electric field (F).

$$E = E^{(0)} - \mu_1 F_1 - \frac{1}{2}\alpha_{ij} F_i F_j - \frac{1}{6}\beta_{ijk} F_i F_j F_k - \frac{1}{24}\gamma_{ijkl} F_i F_j F_k F_l - \ldots \quad (8)$$

Where $E^{(0)}$ is the energy of molecule in the absence of an electronic field, μ is dipole moment vector, α is the linear polarizability of molecule, β and γ are the first and second hyperpolarizabilities, respectively, while i, j and k label the x, y and z components, respectively. It is clear from Eq.1 that the values of μ, α, β, and γ can be obtained by differentiating E with respect to F.

In our present investigation, we have calculated the electronic μ, molecular polarizability, polarizability anisotropy and molecular first hyperpolarizability. For a molecule, the average μ (μ_0) is defined as follows:

$$\mu_0 = \left(\mu_x^2 + \mu_y^2 + \mu_z^2\right)^{\frac{1}{2}} \quad (9)$$

The polarizability (α_0) and its anisotropy (∇a) can be calculated by following equations:

26

$$\alpha_0 = \frac{1}{3}\left(\alpha_{xx} + \alpha_{yy} + \alpha_{zz}\right) \quad (10)$$

$$\Delta\alpha = \left[\left\{\left(\alpha_{xx} - \alpha_{yy}\right)^2 + \left(\alpha_{yy} - \alpha_{zz}\right)^2 + \left(\alpha_{zz} - \alpha_{xx}\right)^2\right\} / 2\right]^{1/2} \quad (11)$$

Similarly, the components of the first hyperpolarizability can be calculated using the following Eq:

$$\beta_i = \beta_{iii} + \sum_{i \neq j}\left[\left(\beta_{ijj} + 2\beta_{jii}\right)/3\right] \quad (12)$$

Using the x, y, z components, and the magnitude of static first hyperpolarizability (β_0) can be calculated by following Eq. 3

$$\beta_0 = \left(\beta_x^2 + \beta_y^2 + \beta_z^2\right)^{\frac{1}{2}} \quad (13)$$

Similarly, the magnitude of the total first static hyperpolarizability (β_{tot}) is calculated calculated using following eq. 6

$$\beta_{tot} = [(\beta_{xxx} + \beta_{xxy} + \beta_{xyy}) + (\beta_{yyy} + \beta_{xxz} + \beta_{yyz}) + (\beta_{xzz} + \beta_{yzz} + \beta_{zzz})]^{½} \quad (14)$$

The first hyperpolarizability (β) is a third rank tensor that can be described by a 3 × 3 × 3 matrix. The 27 components of the 3D matrix can be reduced to 10 components due to the Kleinman symmetry ($\beta_{xyy} = \beta_{yxy} = \beta_{yyx}$, $\beta_{yyz} = \beta_{yzy} = \beta_{zyy}$,… likewise other permutations also take same value). These components have been calculated using Polar = Enonly keyword implemented in GAUSSIAN 09.

The calculation of μ, and polarizabilities, $\boldsymbol{\alpha}$, in Table 3 are the most fundamental electric response properties, which provides a good basis for discussing the reliability of the calculation of the electronic states with various theoretical models in the field of quantum chemistry. The electronic μ for our designed systems is in the range from 2.81 D to 4.94 D. The highest μ is for system 7, which can be attributed to its donor acceptor like structural configuration. The qualitative definition of hardness is closely related to the polarizability, since a decrease of the energy gap usually xx **27**
leads to easier polarization of the molecule[50]. The order of polarizability is as **1** < **4** < **2** < **5** < **7** < **3** = **6** which can be correlated with %IE for corrosion.

Besides this, we have also investigated the potential of our indigenously designed compounds as nonlinear optical (NLO) material by calculating their static first hyperpolarizability and total first hyperpolarizability. The system **7** has the largest values of β_0 and β_{tot}, which are 2732 a.u. and 1639 a.u., respectively. Urea is one of the standard molecules, which are used to study the NLO properties of different materials. The β_0 value of system **7** is about 14 times larger than those calculated value (93.75)[51] of a prototype molecule of urea at same method. The hyperpolarizability values of other molecules are also significant, which indicate that these systems can be also potential candidates for NLO applications.

4. CONCLUSION

Thus, we have calculated different chemical descriptors to investigate the efficiency of titled compounds for corrosion inhibition process. Highest E_{HOMO} value of system **3** is revealing that it would likely more adsorb on the metal surface that can increase the corrosion inhibition efficiency. The binding ability of a molecule with the metal also depends on the electronic charge density on the chelating atom. In the present study, similarly, the substantial charge density on N7 (-0.1518) atom in system **3**, showed that it would lead to the stronger binding ability with metal and easy to bind which would increase the inhibition. The introduction of NO_2 group in system **7**, increases the second peak intensity (at 282 nm) and 40 nm red shift was noticed in the maximum absorption wavelength compared to **1**. **T**he largest ΔN for the **3** as compared to the other investigated compounds showed that it would have improved the inhibition efficiency. Thus, the

higher inhibition of **3** as compared to other systems may be ascribed to the substitution of $–OCH_3$. The greater inhibition efficiency of **2-4** compared to 1, **5-7** is due to the presence of $-CH_3$, OCH_3 and -OH groups in **2-4**, respectively. The electron donor groups ($-OCH_3$, -OH, $-CH_3$) increase the electron density that is also a factor to improve the inhibition efficiency. This study would also help the experimentalists to synthesize new corrosion inhibitors. The significant hyperpolarizability values of studied compounds revealed that these systems would be also potential candidates for NLO applications.

ACKNOWLEDGMENTS

Authors are thankful to the Research Center for Advanced Materials Science, King Khalid University for the support and facilities to carry out the research work

REFERENCES

[1] Umoren, S. A.; Obot, I. B. "**Polyvinylpyrollidone and polyacrylamide as corrosion inhibitors for mild steel in acidic medium**". (2008), Surface Review and Letters (15), 277-286.

[2] Obot, I. B. "**Synergistic Effect of Nizoral and Iodide Ions on the Corrosion Inhibition of Mild Steel in Sulphuric Acid Solution**". (2009), Portugaliae Electrochimica Acta (27), 539-553.

[3] E.E. Ebenso, H. A., S.A. Umoren, I.B. Obot "**Inhibition of Mild Steel Corrosion in Sulphuric Acid Using Alizarin Yellow GG Dye and Synergistic Iodide Additive**". (2008), International Journal of Electrochemical Science (3), 1325 - 1339.

[4] Solmaz, R.; Kardaş, G.; Çulha, M.; Yazıcı, B.; Erbil, M. "**Investigation of adsorption and inhibitive effect of 2-mercaptothiazoline on corrosion of mild steel in hydrochloric acid media**". (2008), Electrochimica Acta (53), 5941-5952.

[5] A.M. Atta, G. A. E.-M., H.S. Ismail, H.A. Al-Lohedan "**Effects of Water Soluble Rosin on the Corrosion Inhibition of Carbon Steel**". (2012), International Journal of Electrochemical Science (7), 11834-11846.

[6] Özcan, M.; Solmaz, R.; Kardaş, G.; Dehri, İ. "**Adsorption properties of barbiturates as green corrosion inhibitors on mild steel in phosphoric acid**". (2008), Colloids and Surfaces A: Physicochemical and Engineering Aspects (325), 57-63.

[7] Bhrara, K.; Kim, H.; Singh, G. "**Inhibiting effects of butyl triphenyl phosphonium bromide on corrosion of mild steel in 0.5 M sulphuric acid solution and its adsorption characteristics**". (2008), Corrosion Science (50), 2747-2754.

[8] Behpour, M.; Ghoreishi, S. M.; Soltani, N.; Salavati-Niasari, M.; Hamadanian, M.; Gandomi, A. "**Electrochemical and theoretical investigation on the corrosion inhibition of mild steel by thiosalicylaldehyde derivatives in hydrochloric acid solution**". (2008), Corrosion Science (50), 2172-2181.

[9] Ramesh, S.; Rajeswari, S. "**Corrosion inhibition of mild steel in neutral aqueous solution by new triazole derivatives**". (2004), Electrochimica Acta (49), 811-820.

[10] Qiu, L.-G.; Xie, A.-J.; Shen, Y.-H. "**A novel triazole-based cationic gemini surfactant: synthesis and effect on corrosion inhibition of carbon steel in hydrochloric acid**". (2005), Materials Chemistry and Physics (91), 269-273.

[11] El Ashry, E. S. H.; El Nemr, A.; Esawy, S. A.; Ragab, S. "**Corrosion inhibitors: Part II: Quantum chemical studies on the corrosion inhibitions of steel in acidic medium by some triazole, oxadiazole and thiadiazole derivatives**". (2006), Electrochimica Acta (51), 3957-3968.

[12] Hassan, H. H.; Abdelghani, E.; Amin, M. A. "**Inhibition of mild steel corrosion in hydrochloric acid solution by triazole derivatives: Part I**". (2007), Polarization and EIS studies. Electrochimica Acta (52), 6359-6366.

[13] Xu, F.; Duan, J.; Zhang, S.; Hou, B. "**The inhibition of mild steel corrosion in 1 M hydrochloric acid solutions by triazole derivative**". (2008), Materials Letters (62), 4072-4074.

[14] Lebrini, M.; Traisnel, M.; Lagrenée, M.; Mernari, B.; Bentiss, F. "**Inhibitive properties, adsorption and a theoretical study of 3,5-bis (n-pyridyl) – 4 – amino - 1,2,4 - triazoles as corrosion inhibitors for mild steel in perchloric acid**". (2008), Corrosion Science (50), 473-479.

[15] Yang, G.; Ying, L.; Haichao, L. "**Experimental studies on the local corrosion of low alloy steels in 3.5% NaCl**". (2001), Corrosion Science (43), 397-411.

[16] Finšgar, M.; Lesar, A.; Kokalj, A.; Milošev, I. "**A comparative electrochemical and quantum chemical calculation study of BTAH and BTAOH as copper corrosion inhibitors in near neutral chloride solution**". (2008), Electrochimica Acta (53), 8287-8297.

[17] Leçe, H. D.; Emregül, K. C.; Atakol, O. "**Difference in the inhibitive effect of some Schiff base compounds containing oxygen, nitrogen and sulfur donors**". (2008), Corrosion Science (50), 1460-1468.

[18] Irfan, A.; Al-Sehemi, A. G.; Al-Assiri, M. S. "**Push–pull effect on the electronic, optical and charge transport properties of the benzo [2,3-b] thiophene derivatives as efficient multifunctional materials**". (2014), Computational and Theoretical Chemistry (1031), 76-82.

[19] Irfan, A.; Al-Sehemi, A. G.; Muhammad, S. "**Push-pull effect on the charge transport properties in anthra [2,3-b] thiophene derivatives used as dye-sensitized and hetero-junction solar cell materials**". (2014), Synthetic Metals (190), 27-33.

[20] Al-Sehemi, A. G.; Irfan, A.; Asiri, A. M. "**Red and yellow color aspects of compound 3 - dicyclopropylmethylene – 5 – dicyanomethylene – 4 – diphenylmethylenetetrahydrofuran – 2 - one: Chromism effect**". (2014), Chinese Chemical Letters (25), 609-612.

[21] Irfan, A. "**First principle investigations to enhance the charge transfer properties by bridge elongation**". (2014), Journal of Theoretical and Computational Chemistry (13), 1450013.

[22] Irfan, A.; Al-Sehemi, A. G.; Al-Assiri, M. S. "**The effect of donors–acceptors on the charge transfer properties and tuning of emitting color for thiophene, pyrimidine and oligoacene based compounds**". (2014), Journal of Fluorine Chemistry (157), 52-57.

[23] Irfan, A. "**Modeling of efficient charge transfer materials of 4, 6-di (thiophen-2-yl) pyrimidine derivatives: Quantum chemical investigations**. (2014)**,** Computational Materials Science (81), 488-492.

[24] Irfan, A. "**Quantum chemical investigations of electron injection in triphenylamine-dye sensitized TiO2 used in dye sensitized solar cells**". (2013), Materials Chemistry and Physics (142), 238-247.

[25] Irfan, A.; Al-Sehemi, A. G.; Al-Assiri, M. S. "**Modeling of multifunctional donor-bridge-acceptor 4, 6-di (thiophen-2-yl) pyrimidine derivatives: A first principles study**". (2013), Journal of Molecular Graphics and Modelling (44), 168-176.

[26] Irfan, A.; Al-Sehemi, A. G.; Kalam, A. "**Structural, electronic and charge transfer studies of dianthra [2,3-b:2′,3′-f] thieno [3,2-b] thiophene and its analogues: Quantum chemical investigations**". (2013), Journal of Molecular Structure (1049), 198-204.

[27] Irfan, A.; Rasool Chaudhry, A.; G. Al-Sehemi, A.; Sultan Al-Asiri, M.; Muhammad, S.; Kalam, A. "**Investigating the effect of acene-fusion and trifluoroacetyl substitution on the electronic and charge transport properties by density functional theory**". (2014), Journal of Saudi Chemical Society, http://dx.doi.org/10.1016/j.jscs.2014.09.009.

[28] Al-Sehemi, A. G.; Irfan, A.; Al-Melfi, M. A. M. "**Highly efficient donor-acceptor hydrazone dyes-inorganic Si/TiO2**

hybrid solar cells". (2015), Spectrochimica Acta Part A: Molecular and Biomolecular Spectroscopy (doi:10.1016/j.saa.2015.02.108.

[29] Guillaumont, D.; Nakamura, S. **"Calculation of the absorption wavelength of dyes using time-dependent density-functional theory (TD-DFT)**. (2000), Dyes and Pigments (46), 85-92.

[30] Al-Sehemi, A. G.; Irfan, A.; Asiri, A. M.; Ammar, Y. A. **"Synthesis, characterization and DFT study of methoxybenzylidene containing chromophores for DSSC materials. Spectrochimica Acta Part A**". (2012), Molecular and Biomolecular Spectroscopy (91), 239-243.

[31] Irfan, A.; Al-Sehemi, A. **"Quantum chemical study in the direction to design efficient donor – bridge - acceptor triphenylamine sensitizers with improved electron injection**". (2012), Journal of Molecular Modeling (18), 4893-4900.

[32] Jin, R.; Irfan, A. **"Theoretical study of coumarin derivatives as chemosensors for fluoride anion**". (2012), Computational and Theoretical Chemistry (986), 93-98.

[33] Irfan, A.; Hina, N.; Al-Sehemi, A.; Asiri, A. **"Quantum chemical investigations aimed at modeling highly efficient zinc porphyrin dye sensitized solar cells**". (2012), Journal of Molecular Modeling (18), 4199-4207.

[34] Al-Sehemi, A. G.; Irfan, A.; El-Agrody, A. M. **"Synthesis, characterization and DFT study of 4H-benzo [h] chromene derivatives**". (2012), Journal of Molecular Structure (1018), 171-175.

[35] Irfan, A.; Ijaz, F.; Al-Sehemi, A.; Asiri, A. **"Quantum chemical approach toward rational designing of highly efficient oxadiazole based oligomers used in organic field effect transistors**". (2012), Journal of Computational Electronics (11), 374-384.

[36] Kohn, W.; Becke, A. D.; Parr, R. G. **"Density Functional Theory of Electronic Structure**". (1996), The Journal of Physical Chemistry (100), 12974-12980.

[37] Shivakumar, S. S.; Mohana, K. N. **"Corrosion Behavior and Adsorption Thermodynamics of Some Schiff Bases on Mild Steel Corrosion in Industrial Water Medium**. (2013), International Journal of Corrosion (2013), 13.

[38] Gece, G. **"The use of quantum chemical methods in corrosion inhibitor studies**". (2008), Corrosion Science (50), 2981-2992.

[39] J.N. Murrell, S. F. K., J.M. Tedder: **"The Chemical Bond**". (1985), John Wiley & Sons, Chichester.

[40] Gao, G.; Liang, C. **"Electrochemical and DFT studies of β-amino-alcohols as corrosion inhibitors for brass**". (2007), Electrochimica Acta (52), 4554-4559.

[41] Khalil, N. **"Quantum chemical approach of corrosion inhibition**". (2003), Electrochimica Acta (48), 2635-2640.

[42] Popova, A.; Christov, M.; Deligeorgiev, T. **"Influence of the Molecular Structure on the Inhibitor Properties of Benzimidazole Derivatives on Mild Steel Corrosion in 1 M Hydrochloric Acid**". (2003), Corrosion (59), 756-764.

[43] Oguike, R. S.; Kolo, A. M.; Shibdawa, A. M.; Gyenna, H. A. **"Density Functional Theory of Mild Steel Corrosion in Acidic Media Using Dyes as Inhibitor: Adsorption onto Fe(110) from Gas Phase**. (2013), ISRN Physical Chemistry, 9.

[44] Khaled, K. F.; Babić-Samardžija, K.; Hackerman, N. **"Theoretical study of the structural effects of polymethylene amines on corrosion inhibition of iron in acid solutions**". (2005), Electrochimica Acta (50), 2515-2520.

[45] C García-Martínez, H. C.-C., J. Escalante-Garcia **"Synthesis and NMR configurational analysis of 1,3 – imidazolidin – 4 - ones derived from (-) - (S) - phenylethylamine**". (2003), Chirality (15), S74-81.

[46] Pearson, R. G. **"Hard and Soft Acids and Bases**". (1963), Journal of the American Chemical Society (85), 3533-3539.

[47] Zhang, D.-q.; Gao, L.-x.; Zhou, G.-d. **"Inhibition of copper corrosion in aerated hydrochloric acid solution by heterocyclic compounds containing a mercapto group"**. (2004), Corrosion Science (46), 3031-3040.

[48] Jacquemin, D.; Preat, J.; Perpète, E. A. **"A TD-DFT study of the absorption spectra of fast dye salts**". (2005), Chemical Physics Letters (410), 254-259.

[49] Srinivasan, P.; Kanagasekaran, T.; Gopalakrishnan, R. **"A Highly Efficient Organic Nonlinear Optical Donor−Acceptor Single Crystal: l-Valinium Picrate**". (2008), Crystal Growth & Design (8), 2340-2345.

[50] Pearson, R. G. **"Absolute electronegativity and hardness: applications to organic chemistry**". (1989), The Journal of Organic Chemistry (54), 1423-1430.

[51] Cassidy, C.; Halbout, J. M.; Donaldson, W.; Tang, C. L. **"Nonlinear optical properties of urea**". (1979), Optics Communications (29), 243-246.